Civil Engineering Infrastructures Journal xx,xx
DOI: 10.22059/ceij.2025.382260.2152

Multi-objective optimization of outriggers and belt walls location in high-rise concrete structures with core-supported and tube-in-tube systems using the Genetic-Descent Gradient integrated method

Safarkhani, M [1], Madhkhan, M [2*]

[1]PhD student, Department of Civil Engineering, Isfahan University of Technology (IUT), University Boulevard, Esteghlal Square, Isfahan, Iran.

Email: m.safarkhani@cv.iut.ac.ir

[2*]Professor, Department of Civil Engineering, Isfahan University of Technology (IUT), University Boulevard, Esteghlal Square, Isfahan, Iran, 983133912511.

Email: madhkhan@iut.ac.ir

Received: 28/09/2024

Revised: 08/01/2025

Accepted: 24/02/2025

Abstract:

As the number of high-rise buildings continues to grow in our modern world, there is an increasing demand for innovative design methods that enable structures to effectively withstand lateral loads. In response, tube structures have emerged as a predominant choice in contemporary high-rise architecture. Nonetheless, the phenomenon of shear lag poses a significant challenge for these systems, often leading to inefficiencies in their performance. To mitigate the effects of shear lag, several construction techniques for tube structures have been devised, particularly the implementation of outrigger and belt wall systems. These systems not only enhance lateral stiffness and reduce shear lag but can also be optimized to address axial shortenings resulting from time-dependent deformations in concrete. This study focuses on optimizing the positioning of outriggers and concrete belt walls in an 80-floor building with core-supported and tube-in-tube structural systems, aiming to minimize lateral displacement and the maximum differential axial shortenings. We employed an integrated approach using the Genetic-Descent Gradient method, which improves the local search capabilities of the genetic algorithm by combining it with the descent gradient technique. Additionally, we applied bounding phase and golden section search methods to further enhance the convergence rate of the algorithm. The findings reveal that lateral displacements and maximum differential axial shortenings in tube-in-tube structures are significantly lower than those in core-supported structures. The combined Genetic-Descent Gradient technique also showed superior performance, as demonstrated by the improved convergence rates compared to the traditional genetic algorithm.

Keywords: *Tall Concrete Structures, Optimization, Outriggers, Genetic Algorithm, Descent Gradient method*

---

1. Introduction

The construction of high-rise buildings has long been recognized as a manifestation of strength and advancement within the construction industry. These structures not only exemplify superior engineering and technological capabilities but also serve as symbols of economic development and growth. As the heights of buildings have increased, the associated technical challenges have multiplied, necessitating the development of new structural systems to effectively resist lateral forces. A novel structural system for high-rise buildings, known as the tubular systems, was introduced, which significantly addresses the challenges associated with structural stability (Khan and Rankin, 1980). This system is characterized by a perimeter framework composed of closely spaced columns, which collectively enables the entire structure to function as a vertical cantilever. As the height of the structure increases, the shear lag effect becomes increasingly pronounced; this phenomenon results in the uneven distribution of lateral forces among the perimeter columns, further accentuating the importance of this design approach in taller buildings. Although tubular systems are highly effective for high-rise constructions, their potential to fully capitalize on the maximum stiffness and strength capacity of the structure is constrained by the shear lag effects prevalent in the perimeter frames. Therefore, while offering substantial advantages in terms of structural performance, these systems require careful consideration to optimize their effectiveness in the context of increasing heights. Research indicates that the incorporation of a belt wall can effectively mitigate the limitations associated with shear lag effects in high-rise buildings (Shin et al., 2012; Arshadi and Kheyroddin, 2019). By facilitating a uniform distribution of stress across the perimeter columns and interconnecting them, the belt wall within this structural system diminishes the shear lag phenomenon. Furthermore, previous studies have shown that the strategic placement of outriggers significantly enhances the overall performance of the structure (Khadka et al., 2023; Habrah et al., 2023; Kamgar and Rahgozar, 2019; Sun et al., 2023; Tavakoli et al., 2022). A simplified methodology was introduced to determine the optimal positioning of outriggers, with the objective of minimizing lateral displacement. This approach involved calculating the top displacement of the structure as the algebraic sum of displacements resulting from external loading and the moment generated by the outrigger. Findings indicated that, under uniform lateral loading conditions, the optimal position for the outrigger is located at a distance of 0.455 times the height of the structure from its top (Taranath, 1975). In a subsequent study, nonlinear time history analysis was employed, and it was discovered that the most favorable performance of the central core and outrigger systems is achieved when the outrigger is positioned at a height of 0.73 times the total height of the structure (Beiraghi and Siahpolo, 2017). These results were corroborated by further research, which recommended the installation of two outriggers at heights of 0.312 and 0.685 times the height of the structure to optimize performance. Additionally, following the installation of an outrigger at the top of the structure, it was determined that the optimal location for a second outrigger is situated at 0.75 times the height of the structure from its apex (McNabb and Muvdi, 1975). Additionally, following the installation of an outrigger at the top of the structure, it was determined that the optimal location for a second outrigger is situated at 0.75 times the height of the structure from its apex (Beiraghi and Hedayati, 2021). The amount of lateral displacement of the structure can be decreased by 15% to 38% for one to four outriggers by installing them in the optimal positions, according to the findings of a study done on a concrete frame with 80-floors and tube-in-tube structural system (Safarkhani and Madhkhan, 2024). An analysis of two buildings with 20 and 25 stories was conducted to ascertain the most effective locations for outriggers. The findings, derived from spectral dynamic analysis and time history analysis, indicated that the optimal outrigger placement was at a distance of 0.38 and a height of 0.5 from the top of the structure, respectively (Haghollahi et al., 2012). A study examined the impact of outriggers on the structural behavior of high-rise buildings. The spectral dynamic analysis demonstrated that positioning an outrigger at the midpoint of the structure resulted in a 56% reduction in maximum lateral displacement. Furthermore, the installation of one outrigger at the top in conjunction with another at the midpoint yielded a 65% reduction in maximum lateral displacement (Putlaiah and Hanuma, 2019). Another investigation revealed that in structures employing a central core system, the lateral displacement could be reduced by up to 35% with the installation of a single outrigger brace. Additionally, the use of two outrigger braces further decreased lateral displacement, achieving reductions of up to 55%. The implementation of outriggers also led to a 45% decrease in story drift compared to structures lacking such systems (Salman et al., 2020). A study utilizing time history analysis indicated that in a building featuring a central core system, the lateral displacement decreased by approximately 15% with the installation of two outriggers located on the 20th and 26th floors (Biradar and Bhandiwad, 2015).

Given the extensive application of meta-heuristics methods in structural engineering, several important studies in this field are reviewed (Hosseini et al., 2024). An Improved Hybrid Growth Optimizer (IHGO) was developed for addressing discrete structural optimization problems, enhancing the original Growth Optimizer (GO), a recent and effective metaheuristic for numerical and real-world optimization (Kaveh and Hamedani, 2024).

In recent years, the evolution of hybrid meta-heuristics—combinations of various optimization algorithms—has significantly enhanced optimization capabilities. A notable example is the integration of Genetic Algorithms (GAs) with local search techniques, such as gradient descent. This combination not only improves convergence speed but also enhances overall solution quality by leveraging the global search capabilities of GAs alongside the efficient local refinement offered by gradient descent methods. Such hybrid approaches have proven effective in solving complex optimization problems in structural design and other fields, making them a promising area of research for further advancements in optimization techniques. However, one of the critical challenges in the gradient descent method is determining the optimal value of the learning rate parameter. Various studies have been conducted in this area to explore effective methods for tuning the learning rate. One of these studies proposes a promising alternative that effectively balances automation and performance. The improvements in convergence speed and generalization could have substantial implications for various applications in machine learning and artificial intelligence. This study provides theoretical explanations for common practices in Stochastic Gradient Descent hyper parameter tuning, including the scaling of learning rates with batch size and the use of high learning rates in certain scenarios. Their method automatically generates a decreasing learning rate during training from a single initial value, thus minimizing manual adjustments and facilitating easier experimentation. They propose a uniform formula for the learning rate, influenced by historical values, which simplifies the tuning process (Song and Yang, 2023). Another study presents a learning-rate-adaptive approach that modifies the learning rate based on empirical estimates of the objective function being minimized. The researchers specifically develop an adaptive variant of the Adam optimizer and apply it to various neural network tasks, particularly for deep learning methods addressing partial differential equations. Their adaptive method consistently reduces the objective function value more rapidly than the standard Adam optimizer with a fixed learning rate. Additionally, the study offers a rigorous convergence proof for the learning-rate-adaptive Stochastic Gradient Descent method applied to a fundamental class of quadratic minimization problems. This proof is based on the analysis of invariant measure laws of Stochastic Gradient Descent and extends to a broader convergence analysis for Stochastic Gradient Descent with random yet predictable learning rates (Dereich et al., 2024).

Given the limited research on multi-objective optimization of three-dimensional structures utilizing tubular structural systems, this study seeks to optimize the configurations of outriggers and concrete belt walls in structures incorporating two tube-in-tube and core-supported systems. While improving efficiency is often a common objective, this research prioritizes the structural security and stability of the buildings through the optimal placement of outriggers and concrete belt walls. By doing so, we aim to demonstrate the critical improvements in lateral displacement and maximum differential axial shortenings, thereby reinforcing the overall safety and integrity of the structure. The primary objective is to minimize the maximum differential axial shortenings in vertical elements, as well as the lateral displacement of the structure. To achieve this, the study employs a combined Genetic Algorithm-Descent Gradient method, enhancing the local search capabilities of the Genetic Algorithm through integration with the descent gradient approach. The results of the optimization processes for both single-objective and multi-objective scenarios are presented, taking into account varying numbers of outriggers, ranging from one to four.

2. Characteristics of the models

This study employs an analytical model, as illustrated in Fig. 1a, to investigate the impact of concrete outriggers and belt walls on tall structures. The configuration consists of 80 floors equipped with two lateral resisting systems: a core-supported system and a tube-in-tube system, which are depicted in Figs. 1b and 1c, respectively. The loading conditions are in accordance with ASCE 7-16 (2016), and seismic analysis is conducted using the dynamic spectral method, with the seismic design category classified as C. To determine the behavior coefficient, a conservative approach is adopted due to the lack of precise values for such structural systems in the design codes. Based on insights from previous studies (Kakde and Desai, 2017; Hong et al., 2010), the behavior coefficient is selected conservatively, without accounting for the potential benefits and effects of tubular performance on the nonlinear behavior of the structure. Specifically, equivalent systems for the tube-in-tube configuration are considered in accordance with the provisions specified in existing design codes. Structural modeling and analysis are conducted following the guidelines of ACI 318-19 (2019) and utilizing the ETABS finite element software. Furthermore, to evaluate the various axial shortenings, the model is analyzed in accordance with CEB-FIP (1990) to estimate the long-term behavior of concrete. Normal cement is employed as the cement type, with an assumed relative humidity of 50%. The construction duration for each floor is established at 7 days, with the dead load of the columns applied 3 days after the casting of the concrete for both the columns and the walls of the structure. The differential axial shortenings are calculated over a 10,000-day period following the completion of the structure. For reinforcement, S400 is utilized for longitudinal reinforcements, while S340 is used for transverse reinforcements. The concrete grade applied to the shear walls, beams, and columns is C60. Furthermore, Table 1 outlines the specifications for the beam and column sections, as well as the thickness of the shear wall core for tube-in-tube and core-supported systems.

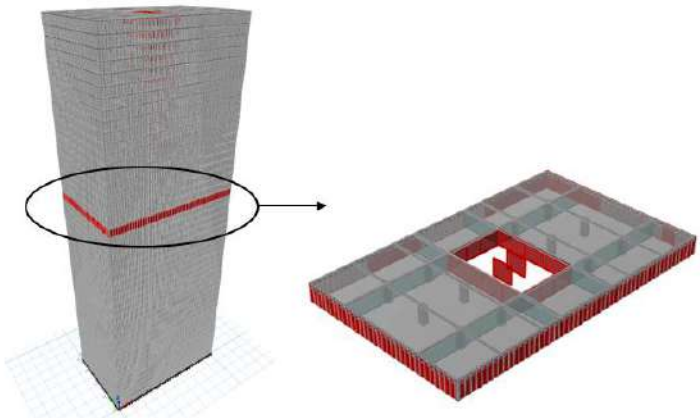

(a) 3D view

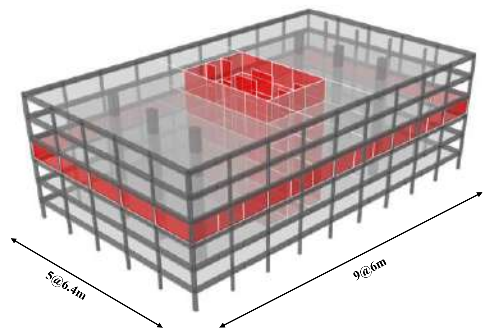

(b) Plan measurements of model with core-supported system

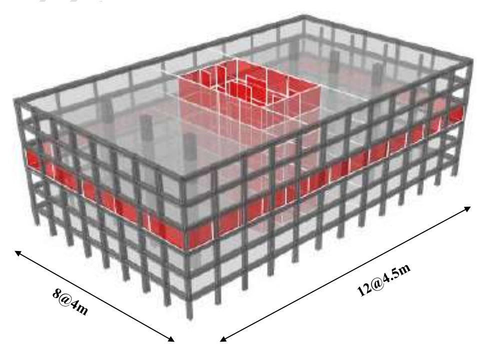

(c) Plan measurements of model with tube-in-tube system

Fig. 1: Analysis models with an outrigger and belt wall.

Table 1.

The cross-sections of beam and columns, as well as the thickness of shear walls for both of tube-in-tube and core-supported systems.

Member	Floor level	Section size width × depth (m x m)		Steel ratio (%)
		Tube-in-tube system	Core-supported system	
Interior Columns	1-20	1.5x1.5	1.7x1.7	3%
	21-40	1.3x1.3	1.6x1.6	3%
	41-60	1.2x1.2	1.4x1.4	3%
	61-80	1.0x1.0	1.2x1.2	3%
Exterior Columns	1-20	1.2x1.2	1.0x1.0	3%
	21-40	1.1x1.1	0.9x0.9	3%
	41-60	1.0x1.0	0.8x0.8	3%
	61-80	0.8x0.8	0.7x0.7	3%
Beams	1-20	0.6x 0.9	0.6x 0.9	-
	21-40	0.6x 0.8	0.6x 0.8	-
	41-60	0.55x 0.7	0.55x 0.7	-
	61-80	0.5x0.65	0.5x0.65	-
Shear walls	1-30	1.0x11.0	1.1x11.0	1%
	31-50	0.8x11.0	1.0x11.0	1%
	51-70	0.7x11.0	0.9x11.0	1%
	71-80	0.6x11.0	0.7x11.0	1%

3. The formulation of optimization problem

The formulation of the optimization problem is represented by Eq. (1).

$$
\begin{aligned}
&Minimize \quad f(x) = \{f_1(x), f_2(x)\} &&\textbf{(1)}\\
&\qquad\qquad f_1(x) = \Delta_{roof} \\
&\qquad\qquad f_2(x) = \max(\delta_1, ..., \delta_N) = \max((u_1^{wall} - u_1^{col}), ..., (u_N^{wall} - u_N^{col})) \\
&Subject\ \ to: \\
&\qquad \theta_i = \frac{\Delta_{k+1} - \Delta_k}{\Delta h_k} \leq 0.02 \\
&\qquad x_{i,\min} \leq x_i \leq x_{i,\max}
\end{aligned}
$$

Where $f_1(x)$ and $f_2(x)$ represent the objective functions for the lateral displacement of the roof and the maximum differential axial shortenings, respectively. x denotes the vector of variables representing the positions of outriggers and wall belts. Δ_{roof} signifies the lateral displacement of the roof, H is the total height of the structure, N is the number of stories, δ_k represents the differential axial shortenings in the kth floor, u_k^{wall} and u_k^{col} denote the vertical displacement of the wall and column in the kth floor, respectively. Δh_k represents the height of the kth floor, Δ_k signifies the lateral displacement in the kth floor, x_{i}, $x_{\text{i,min}}$, and $x_{\text{i,max}}$ denote the position of the ith outrigger, its lowest, and highest possible positions, respectively.

This study utilizes finite element analysis to evaluate the objective functions. In assessing axial shortenings in concrete structures, especially when considering construction sequences and long-term behavior, numerical analysis is favored over analytical equations for determining lateral displacements. For estimating column shortening in concrete structures, the CEB-FIP 1990 guidelines (1990) provide the most effective approach. The equations outlined in this code offer a straightforward and widely accepted method for predicting the long-term behavior of concrete, valued for their simplicity and ease of calculation. Specifically, Eqs. (2) and (3) can be employed to compute the modulus of elasticity and the increase in mean compressive strength, respectively.

$$f_{cm}(t) = \exp\left\{s\left[1-(\frac{28}{t})^{1/2}\right]\right\} \times f_{cm} \tag{2}$$

$$E_{ci}(t) = \left(\exp\left\{s\left[1-(\frac{28}{t})^{1/2}\right]\right\}\right)^{0.5} \times E_{ci} \tag{3}$$

Where E_{Ci} and f_{cm} represent the elasticity modulus of concrete and average compressive strength at the age of 28 days, respectively. t denotes the concrete age in days, and S is the coefficient dependent on the cement type, with a value of 0.25 for normal cement. A linear relationship is established for creep strain and stress when the absolute value of the axial stress is less than 0.4 of the average concrete compressive strength after 28 days. Eq. (4) provides the creep-induced strain at constant stress (t, t_0) in this state (ACI 318-19 (2019)).

$$\varepsilon_{c\sigma}(t,t_0) = E_c(t_0)\left[\frac{1}{E_c(t_0)} + \frac{\phi(t,t_0)}{E_{ci}}\right] = E_c(t_0)J(t,t_0) \tag{4}$$

Where $E_c(t_0)$ reresent the elasticity modulus during the loading, and $1/E_c(t_0)$ represents initial strain per stress unit, and $J(t,t_0)$ is the creep function or the creep function or creep compliance. The notional creep coefficient $\phi(t,t_0)$ is calculated using Eq. (5).

$$\phi(t,t_0) = \left(1+\frac{1-RH/100}{0.46(h/100)^{1/3}}\right).\left[\frac{5.3}{(f_{cm}/10)^{0.5}}\right].\left(\frac{1}{0.1+t_0{}^{0.2}}\right) \\ .\left\{\frac{(t-t_0)}{\left(150\left[1+(1.2\frac{RH}{100})^{18}\right]\frac{h}{100}+250\right)+(t-t_0)}\right\} \tag{5}$$

The shrinkage strain, denoted as $\varepsilon_{cs}(t,t_s)$ is calculated using Eq. (6) (ACI 318-19 (2019)).

$$\varepsilon_{cs}(t,t_s) = \left[160 + 10\,\beta_{sc}(9 - f_{cm}/10)\right] \times 10^{-6} \cdot \left(-1.55\left[1 - \left(\frac{RH}{100}\right)^3\right]\right) \cdot \left[\frac{t - t_s}{0.035h^2 + t - t_s}\right]^{0.5} \quad \textbf{(6)}$$

Where t_0 is the concrete age during the loading in days, t_s is the concrete age in the time of shrinkage commencement which starts by ending the wet curing period, *RH* is the relative humidity of the ambient environment in [%], β_{sc} is the coefficient depending on the used cement type (CEB-FIP 1990, (1990)) which is equal to 5 for normal or rapid curing cement and h is the theoretical dimension of the element in mm, which is obtained from Eq. (7).

$$h = 2A_c/u \quad \textbf{(7)}$$

Where A_c is the cross sectional area and *u* is the perimeter of the member in contact with the atmosphere in [mm].

4. Multi-objective optimization problem

Eq. (8) illustrates the formulation of scalarized objective functions through the weighted sum approach, applied to two conflicting objective functions:

$$\begin{aligned} &Minimize \quad F(x) = \omega\, f_1(x) + (1-\omega)\, f_2(x) \\ &S.t. \qquad\quad x \in Z^n \end{aligned} \quad \textbf{(8)}$$

In this case, *Z* is the set of integer numbers and ω is the weight factor between 0 and 1.

When the weight factor is set to zero, only maximum differential axial shortenings are considered, neglecting the lateral displacement of the structure. Consequently, the optimization results for maximum differential axial shortenings will closely resemble those obtained from single-objective optimization. Conversely, when the weight factor is set to 1, the optimization outcomes for the lateral displacement of the structure will match those of the single-objective function. The optimization process iterates until the weight factor increments to 1 in $\Delta\omega$ intervals, generating numerous Pareto solutions. Furthermore, the lateral displacement and maximum differential axial shortenings are calculated using finite element analysis, where integer design variables denoted as x are employed. The optimization problem is then tackled using the Genetic-Descent Gradient approach, aimed at examining the performance of the Genetic algorithm alongside local search algorithms. In this study, we selected the Genetic-Descent Gradient method as our primary optimization strategy due to its effective balance between exploration and exploitation during the optimization process. The Genetic Algorithm is known for its proficiency in navigating large and complex solution spaces, making it ideal for problems with nonlinear and non-derivative objective functions. However, the Genetic Algorithm often struggles with local search capabilities, which can limit its effectiveness, particularly when fine-tuning solutions is essential. To address this limitation, we combined the Genetic Algorithm with the Descent Gradient method, which improves local search efficiency by focusing on promising regions of the solution space. This hybrid approach facilitates rapid convergence toward optimal solutions and enhances the overall robustness of the optimization process. While each method has its merits, their integration offers a compelling combination of global search capabilities and swift local refinement, making it particularly well-suited for optimizing structural configurations that require careful management of both lateral displacements and differential axial shortenings. This synergy results in faster convergence rates and improved performance in achieving our optimization objectives.

Gradient-based optimization methods are generally unsuitable for addressing the non-constrained nonlinear optimization problem presented in Eq. (1) due to the inclusion of integer variables. These methods typically require objective functions to exhibit continuity and differentiability to facilitate effective minimization. To address this limitation, interpolation techniques can be employed to derive differentiable approximations of the objective functions. In this context, piecewise square interpolation is utilized. By transforming the nonlinear optimization problems characterized by integer variables from Eq. (1) into differentiable nonlinear problems with interpolated polynomial objective functions, they can be reformulated as depicted in Eq. (9):

$$\begin{aligned} &Minimize\ \bar{F}(\tilde{x}) = \omega\, \bar{f}_1(x) + (1-\omega)\, \bar{f}_2(x) \\ &S.t. \qquad \tilde{x} \in R^n \end{aligned} \tag{9}$$

Where *x* is the released vector of X and *R* is the integer numbers series.

4.1. Genetic- Descent Gradient method

The descent gradient method is a widely utilized optimization technique in neural networks, recognized for its effectiveness. This iterative first-order optimization method is employed to identify the minimum or maximum values of a given function. In this study, we propose a hybrid approach that combines the descent gradient method with a genetic algorithm to enhance the local search capabilities of the genetic algorithm, thereby leveraging the strengths of both algorithms to identify a global optimal solution and accelerate convergence. Specifically, the descent gradient method is employed to refine the current optimal solution at the conclusion of each generation of the genetic algorithm. If an improvement is identified during this process, it is carried forward to the subsequent generation. Eq. (10) delineates the search direction utilized at each specific point $x(k)$ when applying the descent gradient method.

$$s(k) = -\nabla f(x(k)) \tag{10}$$

This search direction, which minimizes function values most effectively, is known as the steepest descent method. Eq. (11) outlines the unidirectional search conducted in the negative direction of the derivative. The derivative is computed at the current point to identify the minimum along this direction.

$$\begin{aligned} f(x(k+1)) &= f(x(k) + \alpha(k)s(k)) \\ f(x(k+1)) &= f(x(k) - \alpha(k)\nabla f(x(k))) \end{aligned} \tag{11}$$

The search then advances from the identified minimum point, updating the current point accordingly. The algorithm continues to iterate until a point is located where the gradient exhibits a sufficiently small magnitude. However, a significant challenge for the descent gradient algorithm is determining an appropriate value for α, which represents the learning rate in the aforementioned equations. The following sections will elucidate the methods employed in this study to ascertain the optimal value of α.

4.1.1. Determining the optimal value of the learning rate

Many multivariable optimization algorithms employ consecutive unidirectional search methods to identify the minimum point along a specified search direction. The unidirectional search evaluates function values along this direction to perform a one-dimensional search. Typically, the unidirectional search commences at the point $x(t)$ and progresses in the indicated direction $s(t)$.

This approach implies that points along the search direction $s(t)$—which forms a line in an N-dimensional space and passes through the point $x(t)$—are considered during the search process. Each target point along this search path can be mathematically expressed using Eq. (12).

$$x(\alpha) = x(t) + \alpha s(t) \tag{12}$$

The parameter α is a scalar quantity that defines the relative distance between the point $x(\alpha)$ and $x(t)$. For a given value of α, the corresponding point $x(\alpha)$ can be determined. When α is equal to zero, the point corresponds to the current position $x(t)$. By substituting $x_i(\alpha)$ for each variable x_i and utilizing Eq. (12), one can construct the multivariable objective function as a function of the variable α to identify the minimum point in the specified direction.

The search space for the optimal value of α was bracketed using a bracketing technique, followed by the application of a method for extracting the optimal value within this space. Among the strategies employed in this study to bracket the search space was the bounding phase approach. Subsequently, the golden section search method was utilized to refine the search space and identify the optimal value. A detailed discussion of the bounding phase method and the golden section search approach is presented in the following sections.

The search space for determining the optimal value of α was constrained using a bracketing technique, followed by the application of a method to eliminate portions of the search space. In this study, the bounding phase approach was employed as one strategy to bracket the search space, after which the golden section search method was applied to refine the search space further. A detailed discussion of these methods is provided in the subsequent sections.

- *Bounding phase and golden section search methods*

The minimum of a function can be bracketed using the bounding phase approach. This strategy guarantees the existence of at least one minimum for a single-variable function within the established bracket. As outlined in Eq. (13), the procedure initially estimates the function value at the first guess and employs two evaluations to ascertain the search direction. Subsequently, an exponential search method is utilized to reach the targeted limit.

$$x(k+1) = x(k) + 2^{k}\Delta \tag{13}$$

While bracketing can be executed more swiftly, the accuracy of the bracketed minimum point is compromised due to the large value of Δ. Conversely, a smaller Δ enhances the precision of the bracketing process; however, it may necessitate evaluating additional function values to effectively bracket the minimum point. Following the application of the bounding phase approach to constrain the search space, it is advisable to employ one of the methods for eliminating the search area to locate the minimum. These algorithms operate on the principle of systematically narrowing down the bracketed regions until the optimal solution is attained. Based on the evaluation of function values at two points and the presumption that the function is single-variable within the specified search space, it is possible to conclude that the minimum point cannot be located within a certain region. The methodology for eliminating search areas begins with the consideration of two points, x_1 and x_2, situated within the interval (a,b), such that $x_1 < x_2$. If the function value at x_1 is greater than that at x_2, it indicates that the minimum point x^* cannot lie to the left of x_1, thereby allowing for the elimination of the interval (a,x_1). This action effectively narrows the search range from (a,b) to (x_1,b). Conversely, if $f(x_1) < f(x_2)$, it suggests that the minimum point does not exist within the interval (x_2,b), allowing for the removal of this region as well. In this study, the golden ratio optimization method is utilized as one of the techniques for area elimination. A flowchart illustrating the steps of the Genetic-Descent Gradient method, alongside the bounding phase and golden section search techniques, is presented in Fig. 2.

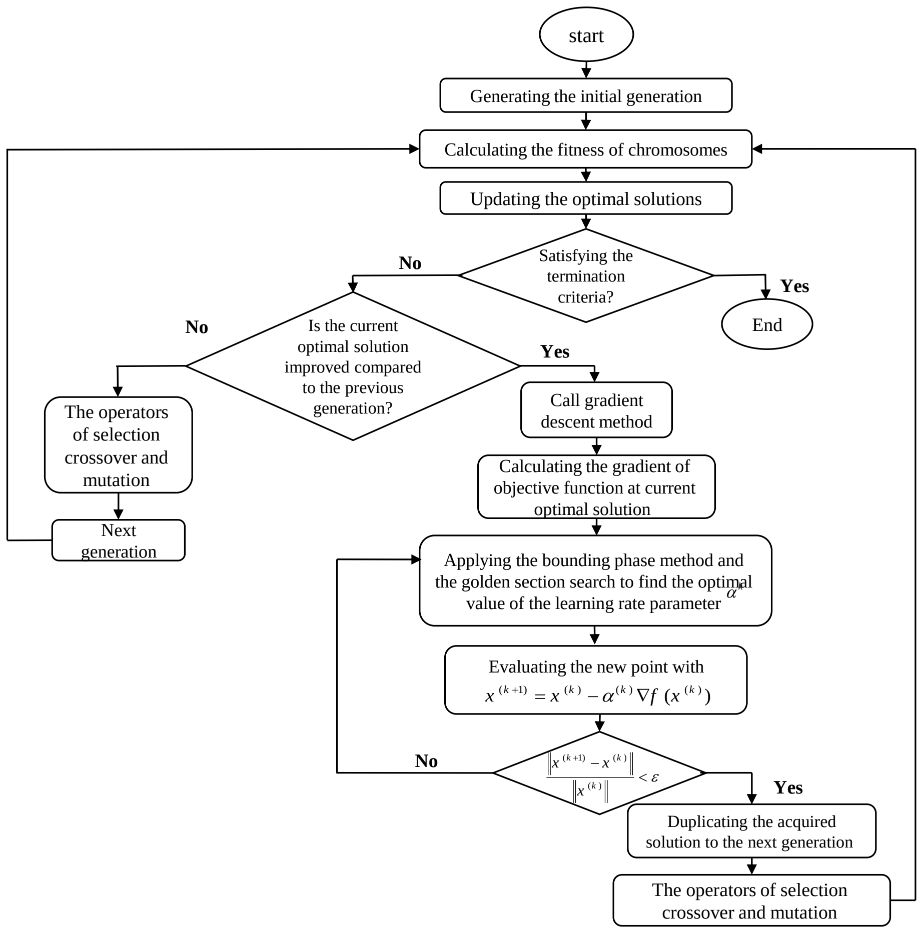

Fig. 2: Flowchart of the steps of Genetic-Descent Gradient algorithm along with two bounding phase and golden section search methods.

5. Optimization results

5.1. Influence of Outriggers and Belt Walls on Lateral Displacement

Before addressing the optimization results, we investigated the effects of outriggers and belt walls on the structure's lateral displacement. The findings, presented in Table 2, detail the maximum lateral displacement for different numbers of outriggers. As indicated in Table 2, the maximum lateral displacement diminishes with an increasing number of outriggers.

Table 2.

Maximum Lateral Displacement for Varying Numbers of Outriggers and Belt Walls.

Configuration	**Lateral displacement (mm)**	
	CSOR	**TinT**
Without outriggers and belt walls	120.7824	93.2566
One outrigger and belt wall	101.4572	77.4029
Two outriggers and belt walls	96.62592	71.8076
Three outriggers and belt walls	91.79462	68.0773
Four outriggers and belt walls	85.75551	64.3471

5.2. Cost Calculation for Outriggers and Belt Walls

Incorporating outriggers and belt walls into structural design presents both advantages and financial implications. Understanding these costs is crucial for effective project budgeting and resource allocation. To assess the economic feasibility of implementing the outrigger and belt wall systems in high-rise concrete structures, we analyzed the costs associated with the materials and labor required to implement outriggers and belt walls compared to traditional reinforcement techniques. Specific cost factors included structural materials such as concrete and steel, formwork, and the added labor for installation of these systems. The calculated costs for the outrigger and belt wall system are detailed in Table 3.

Table 3.

Detailed Cost Calculation for Outriggers and Belt Walls.

	Cost

Materials	Concrete	90-115 $/m^3
	Steel Reinforcement	0.35-0.55 $/kg
	Formwork	0.3-0.75 $/m^2
Labor	-	50-70 $/hour
Design and Engineering Fees	-	5-10% of the total construction costs

In summary, the estimated cost for implementing four outriggers and belt wall systems in an 80-story high-rise building—covering materials, labor, and engineering fees—would be approximately $30,000. The optimized design of the outrigger and belt wall system enhances lateral stiffness and reduces lateral displacements, contributing to lower maintenance costs. Structures with improved lateral load resistance encounter fewer issues related to cracking and deformation, ultimately decreasing the need for expensive repairs. While the initial investment in outriggers and belt walls may be considerable, the advantages of enhanced structural stability and reduced lateral displacement make it a worthwhile investment. To apply a source data table, even if they were taken from the literature.

5.3. Single objective optimization results

The optimization problem is approached by integrating Genetic Algorithm and Descent Gradient methods, utilizing a population size of 150 over 100 generations. After each generation of the genetic algorithm, the descent gradient method is employed if an improvement in the optimal point is observed. This strategy enhances the convergence rate of the genetic algorithm by allowing for the exploration of solutions in the vicinity of the current optimal point. Any improvements achieved through the descent gradient method are subsequently incorporated into the next generation of the genetic algorithm. Prior to conducting multi-objective optimization for an 80-story structural model, single-objective optimization was performed independently for maximum differential axial shortenings and lateral displacements. Figs. 3a and 3b present the results for the 80-story model applying tube-in-tube and core-supported lateral resisting systems, respectively. The results indicate that with the optimal placement of 1, 2, 3, and 4 outriggers and wall belts, the reductions in lateral displacement for the tube-in-tube system are 20%, 31%, 35%, and 37% lower, respectively, compared to the structure without outriggers. Analogous reductions for the core-supported system are noted at 19%, 25%, 32%, and 35%, respectively. Furthermore, the maximum differential axial shortenings of the tube-in-tube system before and after optimization for the four configurations of belt walls and outriggers are recorded as 31%, 39%, 49%, and 55%. The corresponding values for the core-supported system are 31%, 35%, 47%, and 52%. These results clearly demonstrate that the tube-in-tube system achieves a greater rate of reduction in lateral displacement than the core-supported system. Additionally, it is observed that the reduction in the maximum differential axial shortenings objective function is considerable compared to the lateral displacement objective function. However, it is noteworthy that the addition of more belt walls and outriggers results in a diminished reduction rate in both objective functions. It should be noted that the terms “CSOR” and “TinT" refer to the Central Core System with Outrigger and Tube-in-Tube system, respectively.

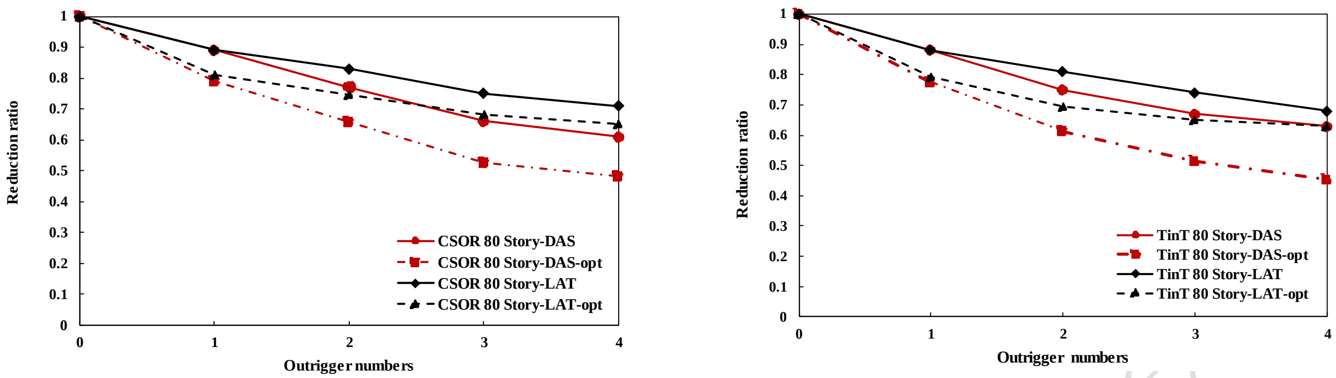

(a) core-supported model

(b) tube-in-tube model

Fig. 3: Normalized values of objective functions before and after optimization for lateral displacement and maximum differential axial shortenings.

5.4. Multi-objective optimization results

Multi-objective optimization was conducted for belt walls and from one to four outriggers. Figs 4a and 4b present the results of the multi-objective optimization process for the Pareto front, as well as for two structural configurations: the core-supported system and the tube-in-tube system. It is observed that reducing the maximum differential axial shortenings leads to an increase in the lateral displacement of the structure.

Moreover, both objective function values decrease as the number of belt walls and outriggers increases. The results of the single-objective optimization are clearly represented at the two ends of the Pareto front in each of the four configurations. Specifically, ω=0 corresponds to the single-objective optimization results for maximum differential axial shortenings, while ω=1 reflects the single-objective optimization results for lateral displacement. As the weight factor increases, the optimal solution for maximum differential axial shortenings gradually supplants the optimal solution for lateral displacement.

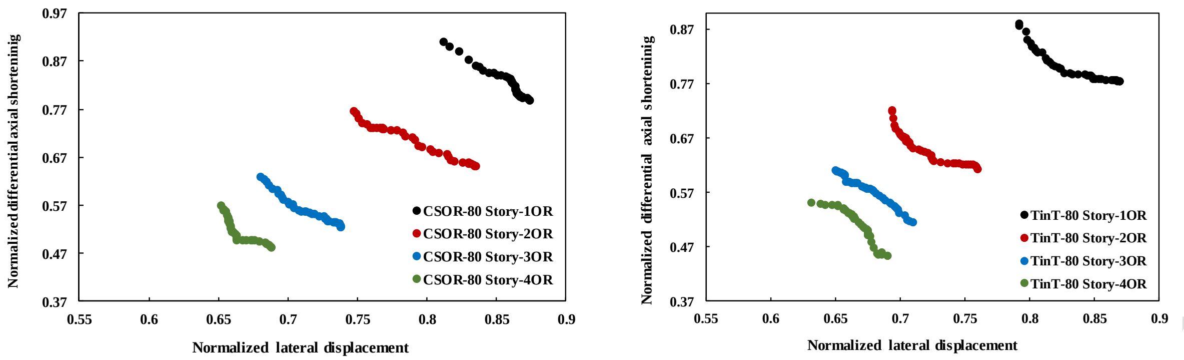

(a) core-supported model

(b) tube-in-tube model

Fig. 4: Pareto-front solutions representing the trade-off between maximum differential axial shortenings and lateral displacement for two models.

5.5. Optimal positions of outriggers and belt walls for the entire set of Pareto-front

Figs. 5 and 6 illustrate the optimal positions for the entire Pareto set across various configurations, including one to four outriggers and belt walls, for structures using core-supported and tube-in-tube lateral systems, respectively. The normalized values of the objective functions, which include lateral displacement and maximum differential axial shortenings, are presented for each configuration. It is observed that as the weight factor increases, the maximum differential axial shortenings decrease while the lateral displacement of the structure increases. Notably, when ω equals zero or one, these values correspond to the outcomes of single-objective optimization for lateral displacement and maximum differential axial shortenings, respectively.

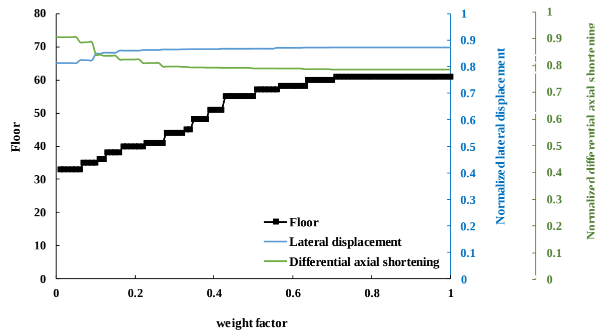

(a) one outrigger-belt wall

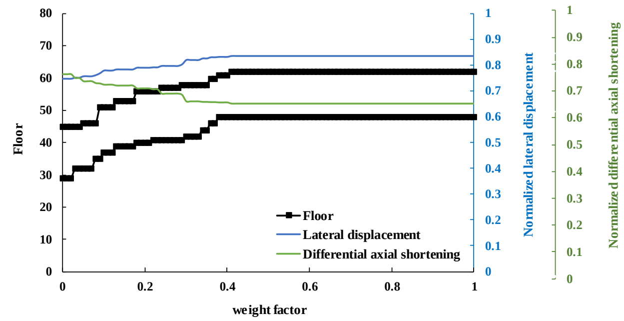

(b) two outriggers-belt walls

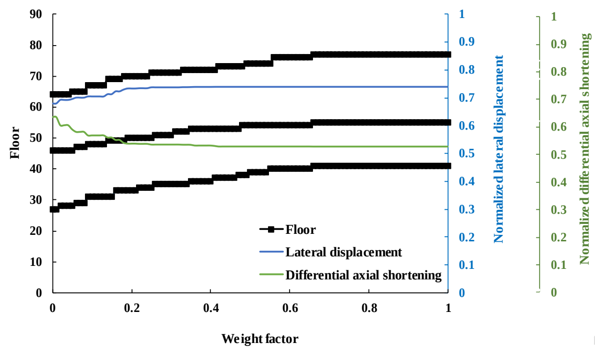

(c) three outriggers-belt walls

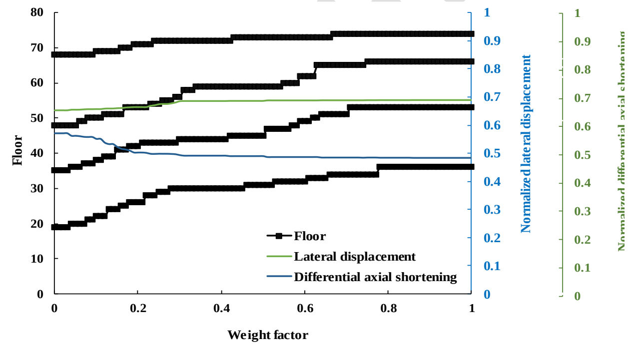

(d) four outriggers-belt walls

Fig. 5: Optimal positioning of outriggers and belt walls within the core-supported structural system for varying weight factors (ω) across one to four outriggers.

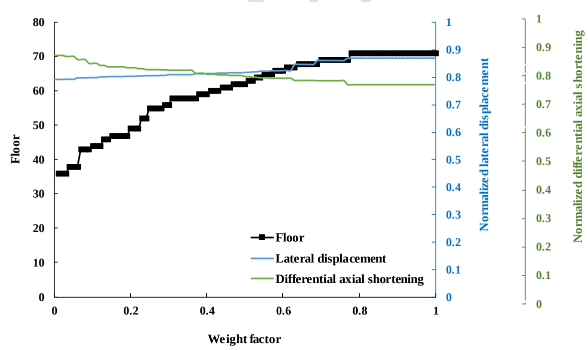

(a) one outrigger-belt wall

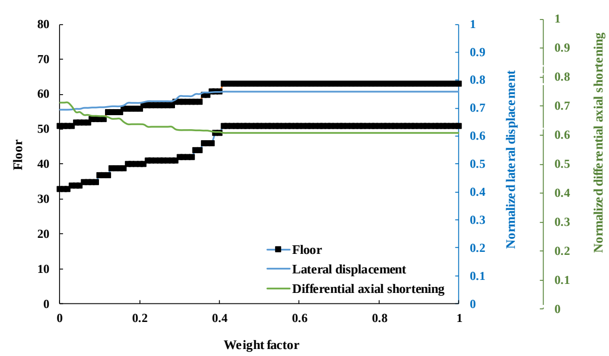

(b) two outriggers-belt walls

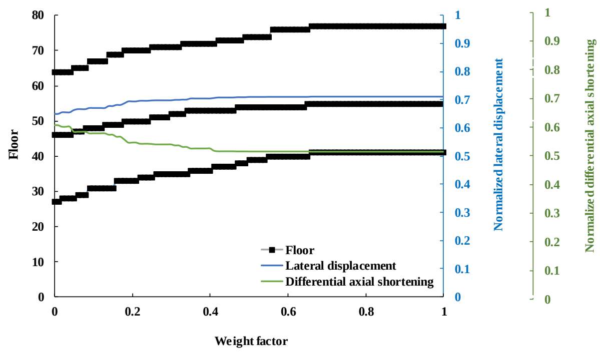

(c) three outriggers-belt walls

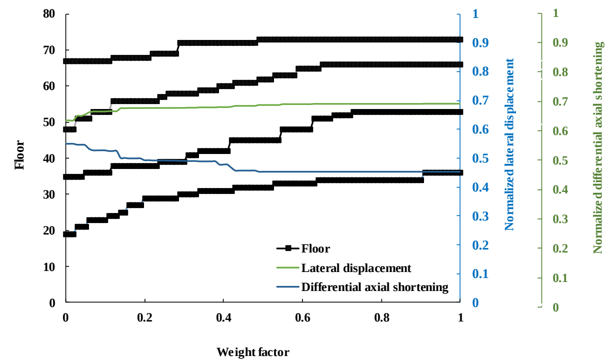

(d) four outriggers-belt walls

Fig. 6: Optimal positioning of outriggers and belt walls within the tube-in-tube structural system for varying weight factors (ω) across one to four outriggers.

6. Comparison of the convergence of Genetic algorithm and Genetic-Descent Gradient algorithm

The optimization problem in this study was addressed using a Genetic Algorithm (GA), selected for its ability to explore vast search spaces and its flexibility in handling optimization problems with discontinuous and non-derivative objective functions. However, due to the inherent limitations of the GA in local search, it was combined with the descent gradient method, a local search technique. This combination allows for circling around current optimal points during each iteration of the GA, thereby accelerating convergence rates. Furthermore, enhancing the learning rate parameter through the bounding phase and golden section search approaches contributed to a faster convergence rate in the descent gradient method. Fig. 7 shows the convergence curves for Genetic Algorithms and Genetic-Gradient Descent algorithms. The convergence curve for the Genetic-Gradient Descent method is plotted once using both the Bounding Phase and Golden Section Search methods, and once without employing these two methods. It is important to note that the terms "GA-GRADIENT (Simple)" and "GA-GRADIENT (Combined)" refer to the Genetic-Gradient Descent method in its simple form (without the Bounding Phase and Golden Section Search methods) and in its combined form (with these methods), respectively. The results indicate that each model experiences rapid convergence during the early stages of the optimization process, followed by stable convergence in the later stages. Specifically, for a structure with one outrigger and a belt wall, convergence occurs by generation 50 when using the Genetic Algorithm. The corresponding values for structures with two, three, and four outriggers and belt walls are 48, 37, and 53, respectively. In contrast, the Simple Genetic-Gradient Descent algorithm converges at generations 46, 45, 34, and 43, while the Combined Genetic-Gradient Descent achieves convergence at generations 32, 27, 29, and 41 for similar configurations. The results indicate that the Composite Genetic-Gradient Descent method performs better than both the Genetic Algorithm and the Simple Genetic-Gradient Descent method, demonstrating a higher convergence speed. Therefore, by combining the two methods, the Bounding Phase and Golden Section Search, with the Gradient Descent method, a better performance is achieved. As outlined in our findings, the optimal selection of the α parameter using both the Bounding Phase and Golden Section Search methods has significantly increased the convergence speed of the Genetic-Gradient Descent method. This improvement reflects the effectiveness of incorporating these methods into our optimization framework, which allows for a more precise adjustment of the alpha parameter, leading to faster and more stable convergence.

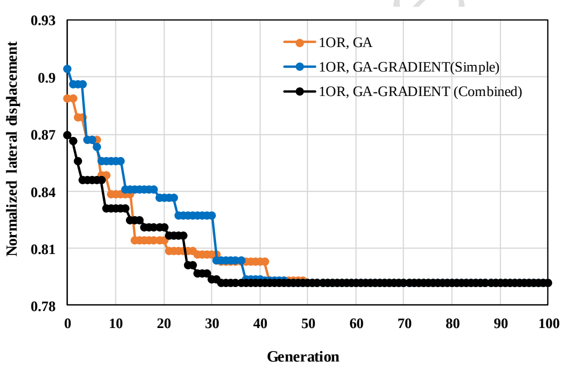

(a) one outrigger-belt wall

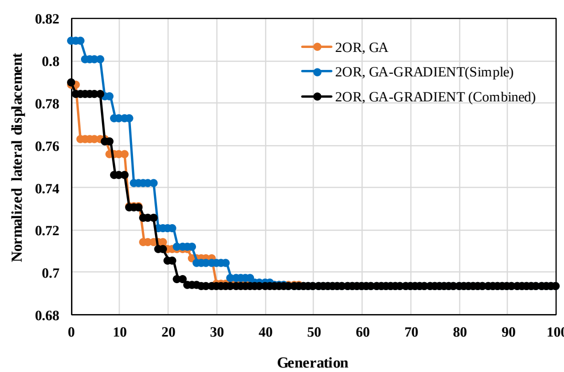

(b) two outriggers-belt walls

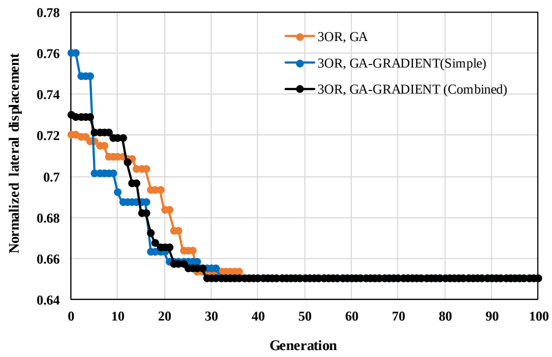

(c) three outriggers-belt walls

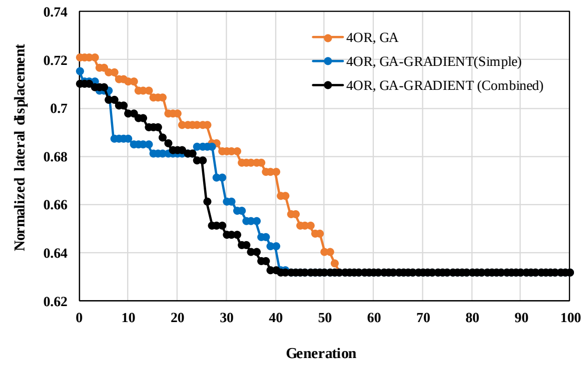

(d) four outriggers-belt walls

Fig. 7: Convergence curve of lateral displacement with two methods of Genetic algorithm and Genetic-Gradient Descent for 1-4 outriggers and belt walls.

7. Conclusion

This study utilized the integrated Genetic-Descent Gradient method to optimize the positions of outriggers and concrete belt walls, aiming to minimize lateral displacement and maximum differential axial shortenings in two structural systems: core-supported and tube-in-tube. The optimization results for a 3D, 80-story building indicate that the core-supported system experiences greater lateral displacement compared to the tube-in-tube system. This difference can be attributed to the tube-in-tube system's more uniform behavior, which is facilitated by its closely spaced perimeter columns that enhance the structural elements' ability to cooperate effectively against lateral loads. When additional belt walls and outriggers were incorporated into the core-supported system, the reduction in lateral displacement occurred more rapidly than in the tube-in-tube system. This enhanced reduction could be due to the optimal connection achieved between the exterior tube and the central core at the appropriate number of outriggers, leading to greater reductions in lateral displacement compared to the tube-in-tube structure. The tube-in-tube system exhibits a more uniform force distribution in its perimeter columns, resulting in lower maximum differential axial shortenings than those observed in the core-supported system. Furthermore, the combined Genetic-Descent Gradient method improved the convergence rate of the Genetic Algorithm by better balancing exploration and exploitation. By selecting the current optimal solution from each generation of the Genetic Algorithm as the starting point for the descent gradient method, the speed of convergence was enhanced, as the choice of the starting point is critical for reaching the global optimal solution. The learning rate parameter also plays a significant role in the effectiveness of the descent gradient approach. Therefore, determining the optimal learning rate through bounding phase and golden section search methods is essential for maintaining the continuity of the descent gradient method in the local optimum. Overall, the combination of stochastic optimization techniques, such as the Genetic Algorithm, with local search algorithms like the descent gradient method has been shown to accelerate convergence significantly.

On behalf of all authors, the corresponding author states that there is no conflict of interest.

References

ACI Committee. (2019). *Building code requirements for structural concrete (ACI 318-19) and commentary*. American Concrete Institute.

ASCE. (2016). *Minimum design loads for buildings and other structures*, American Society of Civil Engineers.

Arshadi, H. and Kheyroddin, A. (2019). “Shear lag phenomenon in the tubular systems with outriggers and belt trusses”. *Magazine of Civil Engineering*, 2 (86), 105-118. https://doi.org/10.22124/jcr.2020.13137.1362

Beiraghi, H. and Hedayati, M. (2021). “Optimum location of second outrigger in RC core walls subjected to NF earthquakes”. *Steel and Composite Structures, An International Journal*, 38(6), 671-690.

https://doi.org/10.12989/scs.2021.38.6.671

Beiraghi, H. and Siahpolo, N. (2017). “Seismic assessment of RC core-wall building capable of three plastic hinges with outrigger”. *The Structural Design of Tall and Special Buildings*, 26(2), 1306.

https://doi.org/10.1002/tal.1306

Biradar, P.N. and Bhandiwad, M.S. (2015). “A performance based study on static and dynamic behaviour of outrigger structural system for tall buildings”. *International Research Journal of Engineering and Technology (IRJET)*, 2(05), 2395-0072.

Code, CEB-FIP Model. (1990). "Comité Euro-International du Béton (CEB), 1993."

Dereich, S., Jentzen, A. and Riekert, A. (2024). “Learning rate adaptive stochastic gradient descent optimization methods: numerical simulations for deep learning methods for partial differential equations and convergence analyses”. *arXiv preprint arXiv:2406.14340*.

https://doi.org/10.48550/arXiv.2406.14340

Habrah, A., Batikha, M. and Vasdravellis, G. (2022). “An analytical optimization study on the core-outrigger system for efficient design of tall buildings under static lateral loads”. *Journal of Building Engineering*, 46, 103762.

https://doi.org/10.1016/j.jobe.2021.103762

Haghollahi, A., Ferdous, M.B. and Kasiri, M. (2012). “Optimization of outrigger locations in steel tall buildings subjected to earthquake loads”. *In The 15th World Conference on Earthquake Engineering*, Lisboa.

Hong, W.K., Park, S.C., Lee, H.C., Kim, J.M., Kim, S.I., Lee, S.G. and Yoon, K.J. (2010). “Composite beam composed of steel and precast concrete (modularized hybrid system). Part III: Application for a 19-storey building”. *The Structural Design of Tall and Special Buildings*, 19(6), 679-706.
https://doi.org/10.1002/tal.507

Hosseini, P., Kaveh, A., Fathali, M.A. and Hoseini Vaez, S.R. (2024). “A two-loop RBDO approach for steel frame structures using EVPS, GWO, and Monte Carlo simulation”. *Mechanics of Advanced Materials and Structures*,1-20.
https://doi.org/10.1080/15376494.2024.2352800

Kakde, P.A. and Desai, R. (2017). “Comparative study of outrigger and belt truss structural system for steel and concrete material”. *IRJET Journals*, 4(5).

Kamgar, R. and Rahgozar, P. (2019). “Reducing static roof displacement and axial forces of columns in tall buildings based on obtaining the best locations for multi-rigid belt truss outrigger systems”. *Asian Journal of Civil Engineering*, 20, 759-768.
https://doi.org/10.1007/s42107-019-00142-0

Kaveh, A. and Hamedani, K.B. (2024). “A hybridization of growth optimizer and improved arithmetic optimization algorithm and its application to discrete structural optimization”. *Computers & Structures*, 303, 107496.

https://doi.org/10.1016/j.compstruc.2024.107496

Khadka, S., Khadka, T.B., Magar, R.T. and Rawat, B. (2023). "Behavior and optimum location of outrigger and belt truss system in high-rise buildings subject to seismic loading". *SCITECH Nepal*, 17(1), 12-30.
https://doi.org/10.3126/scitech.v17i1.60465

Khan, F.R. and Rankine, J. (1980). "Tall building systems and concepts". *ASCE*.

McNabb, J.W. and Muvdi, B.B. (1975). "Drift reduction factors for belted high-rise structures". *Engineering Journal*, 12(3), 88-91.
https://doi.org/10.62913/engj.v12i3.247

Putlaiah, B. and Hanuma, P. (2019). "Comparative study of usage of outriggers and belt truss system for high-rise concrete buildings". *International Journal of Research in Engineering and Technology*, 6(09), 865-872.

Safarkhani, M. and Madhkhan, M. (2024). "Multi-objective optimization design of concrete outriggers based on Genetic–HookeJeeves algorithm: Reducing lateral deflection, differential axial shortening, and construction cost of the structure". *The Structural Design of Tall and Special Buildings*, 33(16), e2157.
https://doi.org/10.1002/tal.2157

Salman, K., Kim, D., Maher, A. and Latif, A. (2020). "Optimal control on structural response using outrigger braced frame system under lateral loads". *Journal of Structural Integrity and Maintenance*, 5(1), 40-50.
https://doi.org/10.1080/24705314.2019.1701799

Shin, M., Kang, T.H.K., LaFave, J.M. and Grossman, J.S. (2012). “Design and behaviour of reinforced concrete high-rise tube building with belt walls”. *The Structural Design of Tall and Special Buildings*, 21(12), 918-932.
https://doi.org/10.1002/tal.661

Song, Z. and Yang, C. (2023). “An automatic learning rate schedule algorithm for achieving faster convergence and steeper descent”. *arXiv preprint arXiv*:2310.11291.
https://doi.org/10.48550/arXiv.2310.11291

Sun, F.F., Yu, R.J. and Jia, R.Z. (2023). “Practical optimal design method for multi-outrigger building structures under inter-story drift constraints”. *Advances in Structural Engineering*, 26(2), 381-395.
https://doi.org/10.1177/13694332221127341

Taranath, B.S. (1974). “Optimum belt truss locations for high-rise structures”. *Engineering Journal*, 11(1), 18-21.
https://doi.org/10.62913/engj.v11i1.221

Tavakoli, H., Moradi, M., Goodarzi, M., & Najafi, H. (2022). "Outrigger braced system placement effect on seismic collapse probability of tall buildings". *Civil Engineering Infrastructures Journal*, 55(2), 259-276.
https://doi.org/10.22059/ceij.2022.319629.1744